

C H A P T E R IX

CHEMICAL DISSOLUTION OF CALCITE CLEAVAGES  
IN AQUEOUS SOLUTIONS OF L(+) TARTARIC ACID

## CHAPTER IX

### CHEMICAL DISSOLUTION OF CALCITE CLEAVAGES IN AQUEOUS SOLUTIONS OF L(+) TARTARIC ACID

	PAGE
9.1 INTRODUCTION ... ..	143
9.2 EXPERIMENTAL ... ..	144
9.3 OBSERVATIONS AND RESULTS ...	145
9.3.1 CHARACTERISTICS OF ETCH PITS ...	145
9.3.1.1 EFFECT OF ETCHING TIME ON ETCH PITS BY KEEPING ETCHING TEMPERATURE AND ETCHANT CONCENTRATION FIXED	146
9.3.1.2 EFFECT OF ETCHANT CONCENTRATION ON ETCH PITS AT CONSTANT ETCHING TIME AND TEMPERATURE ...	147
9.3.1.3 EFFECT OF ETCHING TEMPERATURE ON ETCH PITS PRODUCED BY A FIXED ETCHANT CONCENTRATION AND ETCHING TIME	147
9.3.2 CALCULATION OF ETCH RATES ...	148
9.3.2.1 TIME-DEPENDENT ETCH RATES ...	148
9.3.2.2 CONCENTRATION-DEPENDENT ETCH RATES	149
9.3.2.3 TEMPERATURE-DEPENDENT ETCH RATES	150
9.4 DISCUSSION ... ..	151
9.4.1 QUALITY OF ETCH PITS ...	153
9.4.2 MAXIMA IN ETCH RATES VERSUS CONCENTRATION PLOTS ...	154

	PAGE
9.4.3 REACTION PRODUCT INHIBITION ...	157
9.4.4 IMPORTANCE OF ACTIVATION ENERGY	158
9.4.5 ELECTROLYTIC CONDUCTIVITY OF ETCHANT	160
9.4.6 VISCOSITY OF ETCHANT ...	162
9.4.7 MECHANISM OF DISSOLUTION ...	163
9.5 CONCLUSIONS ...	164

TABLES

FIGURES

REFERENCES

## 9.1 INTRODUCTION:

Applications of selective etching as a tool in the study of dislocation behaviour are well demonstrated /1/. However, the basic mechanism of the process is not yet fully understood. Since the classical work of Gilman et al./2/, much work in this direction has appeared in the literature on alkali halides /3-9/ as well as on metals /10-12/ in which attempts have been made to understand it. Excellent account on etching of crystals is now available /13-15/.

Etching solutions of alkali halides consists of a solvent (usually some alcohol or organic acid) to which an inhibitor is added. The etchants for metals and semiconductors are relatively complicated and consists of atleast two solutions. One of these solutions forms a compound with crystals while the other desorbs it by forming certain complexes. There is another class of etchants which consists of some pure solutions, for example, mineral acids, strong alkalies for etching of calcite, fluorite, barite, magnesium oxide, etc. This class of etchant is also suitable for the study of the etching process.

The shape of an etch pit is dependent on the nature, concentration and temperature of an etchant. Occurrence of different shapes of etch pits on calcite cleavage faces due to various types of etchants and their different concentrations are reported /16-22/. In all cases the diluent used to change concentration of an etchant was distilled water in which calcite is sparingly soluble (0.008 gm per litre at 20°C). It is thus clear that with the same etchant, either concentrated or diluted, the chemical reaction is not materially changed. However, the rate of reaction on cleavage face of calcite changes, which in some cases gives rise to production of etch pits

of various shapes. This obviously points to the unusual physical, chemical and crystallographic characteristics of calcite in general and its cleavages in particular. It was also reported that even with the same concentration of an etchant, the rate of stirring of the solution has a marked effect on shape/or eccentricity of etch figures /23,19/.

The present author has carried out a detailed systematic study of etch rates on calcite cleavages by employing optically active etchant L(+) tartaric acid (or d-tartaric acid, dextro-rotatory). Doubly distilled water was used as a solvent. This etchant is a dislocation etchant. The present work reports optical study of etch rates on calcite cleavages as a function of etching time, etchant concentration, etching temperature, etchant viscosity and electrolytic conductivity of aqueous solution of L(+) tartaric acid.

## 9.2 EXPERIMENTAL:

Natural crystals of calcite were obtained from various localities in India (Shivrajpur, Pavagadh, Broach from Gujarat State and Rajasthan, etc.). The crystals are fairly big with their sizes ranging from 1 cm to 15 cm with cross-sectional area of the order of 3 x 3 cm. A big crystal was selected and etching work was carried out on small pieces obtained by cleaving the crystal in the usual way, i.e., by giving a sharp blow with a hammer on a razor blade kept in contact with the crystal along cleavage direction. The cleavage surface was fully immersed in a still etchant of known concentration for desired time of etching at a constant temperature. The temperature of the etchant was maintained to within  $\pm 0.5^{\circ}\text{C}$  by a regulator attached to constant temperature water bath for studies at higher temperature and by ice for studies at lower temperatures. After etching the crystal for a given period, it was kept in running water for some time. It was then dried by hot air blower. The samples etched were optically studied by CZ VERTICAL microscope

described in chapter II. The variation of etch pit dimensions along directions  $[110]$  and  $[\bar{1}\bar{1}0]$  were carried out by using filar micrometer eyepiece (750x with least count of 0.2 microns). An accuracy of  $\pm 0.1 \mu$  can be achieved by this method. The surface dissolution rate was measured by usual weight loss method using a semi-micro-balance. Electrical conductivity of etching solution was measured using a resistance bridge supplied by Philips, India (model PR-9500) described in chapter II. Viscosity at various etching temperatures was determined by Ostwald viscometer. For determining viscosity at high temperatures, data on thermal expansion and density of etchant at different temperatures was obtained by fabricating a volume dilatometer.

### 9.3 OBSERVATIONS AND RESULTS:

Aqueous solutions of A.R. quality L(+) tartaric acid of varying concentrations were prepared at room temperature and freshly cleaved faces of calcite crystal were subjected to etching by the above solution for different etching times/and different temperatures. In what follows, the terms etchant and aqueous solution of L(+) tartaric acid are used to have the same meaning. The crystal was then washed with running distilled water and dried by hot air blower. It was then examined under optical microscope.

#### 9.3.1 Characteristics of Etch Pits:

The etch pits on a cleavage face of calcite produced by L(+) tartaric acid solution are basically of two types: (i) Pyramidal etch pits, and (ii) flat-bottomed etch pits with plane triangular shape on the face under observation. The line of symmetry of these pits is along  $[110]$  and the vertices of the triangular pits and percussion star are collinear, i.e., they are on  $[110]$ . The triangular base is along  $[\bar{1}\bar{1}0]$  perpendicular to  $[110]$ , i.e., line of symmetry. A typical photomicrograph of an etch pit on cleavage face is shown

in table 9.1 alongwith tracing of percussion star and etch pits produced by different concentrations of L(+) tartaric acid at 50°C depicting the above features. In order to study the effects of etching time, etching temperature and etchant concentrations, experiments were carried out by keeping two of the above factors constant. The observations based on optical study of several pairs of oppositely matched cleavage faces are as under.

#### 9.3.1.1 Effect of etching time on etch pits by keeping temperature and etchant concentration fixed:

Etching time is one of the important factors contributing to successful controlled dissolution and attendant appearance of structure enabling their detailed study possible with the help of optical techniques, e.g., if etching time is short as compared to that appropriate for a particular material, the etch structure will not be completely developed nor will there be sufficient details revealed to permit accurate interpretation of the etched portions on a crystal face. Too long etching time is just as unsatisfactory as one too short. This is connected directly with the disclosing of details of surface structure to different degrees. It should also be noted that if these points are not properly considered, some part of the revealed structure may be completely obliterated. Further, condition of surface such as freshly cleaved surface, heat-treated surface, mechanically treated surface, radiation affected surface, etc., also affects not only the etching time and etching temperature but also concentration and composition of etchant. Hence for obtaining consistent results, it is necessary to carry out etching at constant time or within a specified range of etching times. The following are the results of etching fresh calcite cleavage faces at constant temperature and concentration of L(+) tartaric acid solution.

- (i) With the increase in etching time the number and location of etch pits with plane shape triangle remain unchanged, but the pits grow in size.

- (ii) The cleavage lines are etched away by successive etching /24-26/.
- (iii) As a result, there is a shifting of cleavage line from its original position on the virgin unetched cleavage surface.
- (iv) Optical examination of simultaneously etched oppositely matched cleavage counterparts under identical periods of etching has indicated almost perfect one-to-one correspondence of etch patterns (e.g., etch pits, etch grooves, etc.).

#### 9.3.1.2 Effect of etchant concentration on etch pits at constant etching time and temperature:

Etchant concentration is a factor which governs etch rate at preferential spots on an otherwise seemingly perfect crystal face. At a fixed etching time and temperature, the concentration of L(+) tartaric acid was varied from 0.025 to 0.2 M and the etch patterns produced on a cleavage face of calcite were optically studied. The following are the results:

- (i) The density of etch pits on cleavage counterparts of calcite, for different etchant concentrations and at constant etching temperature and etching time has remained practically unchanged.
- (ii) With increase in etchant concentration, the dimensions of plane shape of etch pits on cleavage face increase. The basic plane shape remains a triangle. This is also true for the direction of line of symmetry. However elongated, short and curvilinear triangles were observed for different etchant concentrations.

#### 9.3.1.3 Effect of etching temperature on etch pits produced by a fixed etchant concentration and etching time:

Etching temperature is one of the important factors influencing the reaction rate and a surface under study. The precise influence of temperature varies with the composition and concentration of etchant, amount of impurity natural or intentionally added and

previous history of the specimen. Hence for reproducible results, etching experiments should be carried out at constant temperature. The general observations are as follows:

- (i) At lower and higher temperatures the density of triangular etch pits on oppositely matched cleavage counterparts remains practically the same. The range of etchant temperature is from 15°C to 50°C.
- (ii) The pits grow in size at elevated temperature and sometimes they coalesce and form a bigger etch pit.
- (iii) There is almost one-to-one correspondence of etch pits on oppositely matched cleavage counterparts etched at different etching temperatures.

The above qualitative observations on triangular etch pits presented in table 9.1 were quantified by considering the increase in the dimensions of plane shape of etch pits.

### 9.3.2 Calculation of etch rates:

#### 9.3.2.1 Time-dependent etch rates:

The lengths of triangular etch pits increase with etching time for a fixed etchant concentration and constant etching temperatures. Hence the increase in etch pit lengths along  $[110]$  and  $[\bar{1}\bar{1}0]$  was systematically studied by measuring them by a filar micrometer eyepiece. Further, with increase in etching the surface material was eaten away. Hence weight loss per  $\text{cm}^2$  was calculated in the usual way. Table 9.2 presents a typical set of observations on length (L) and breadth (B) of an etch pit measured along directions  $[110]$  and  $[\bar{1}\bar{1}0]$  respectively and weight loss per  $\text{cm}^2$  with etching time at various etching temperatures using different concentrations ranging from 0.025 to 0.2 M of aqueous solution of L(+) tartaric acid as etchants. Fig.9.1 presents the plots of etch pit lengths and breadths along directions  $[110]$  and  $[\bar{1}\bar{1}0]$  respectively and

etching time. It is clear from the plots that length and breadth of an etch pit varies linearly with etching time and the straight line passes through the origin. The slopes of these lines give the rate of tangential dissolution,  $V_{tL}$  along  $[110]$  and  $V_{tB}$  along  $[\bar{1}\bar{1}0]$  at corresponding etching temperature. Similarly, weight loss per  $\text{cm}^2$  is plotted against etching time (Fig. 9.2); the plots are again straight lines passing through origin. The slopes of these plots give the rate of surface dissolution,  $V_s$  in  $\text{gm}\cdot\text{cm}^{-2}$  per unit time. On dividing this quantity by density of calcite ( $2.71 \text{ gm/cc}$ ) one gets the rate of surface dissolution,  $V_s$  in  $\text{cm}\cdot\text{sec}^{-1}$ . It should be mentioned here that the plots of length (L) and breadth (B) of an etch pit and weight loss per  $\text{cm}^2$  are always straight lines for all concentrations and etching temperatures of L(+) tartaric acid solutions. Straight line plots indicate that rates of tangential as well as surface dissolution are independent of etching time but depend on temperature and concentration of the etchant.

#### 9.3.2.2 Concentration-dependent etch rates:

The dependence of tangential rate ( $V_{tL}$ ,  $V_{tB}$ ) and surface dissolution rate ( $V_s$ ) on concentration of L(+) tartaric acid solution at various etching temperatures is illustrated by Figs.9.3 and 9.4 respectively. The values of  $V_{tL}$ ,  $V_{tB}$  and  $V_s$  for various concentrations and temperatures are listed in table 9.3. A careful examination of Figs.9.3 and 9.4 shows that rate of tangential dissolution and that of surface dissolution increase initially with increase in concentration of the L(+) tartaric acid solution. They attain maximum values given by:

- (i) Points A,B,C,D,E corresponding to maximum values of tangential dissolution rate along length direction  $[110]$ , namely,  $V_{tLP}$  (Fig.9.3) at etchant concentration 0.075 M.
- (ii) F,G,H,I,J corresponding to maximum values of tangential dissolution rate along breadth direction  $[\bar{1}\bar{1}0]$ , namely,  $V_{tBP}$  (Fig.9.3) at etchant concentration 0.075 M.

(iii) K,L,M,N,O corresponding to maximum surface dissolution rate, namely,  $V_{SP}$  at etchant concentration 0.075 M (Fig.9.4).

The rate of dissolution then decreases at higher concentration of L(+) tartaric acid solutions. The nature of  $V_{tL}$ -C,  $V_{tB}$ -C and  $V_S$ -C curves are similar. The maximum rate ( $V_{tLP}$ ,  $V_{tBP}$  and  $V_{SP}$ ) is observed at 0.075 M concentration at all etching temperatures. This indicates that the concentration corresponding to maximum rate of reaction does not depend upon etching temperature. In what follows the concentration at peak value of etch rate will be referred to as  $C_P$  (=0.075 M). It is interesting to note that although  $C_P$  has the same value for maximum tangential rates along  $[110]$  and  $[\bar{1}\bar{1}0]$  and surface dissolutions, the magnitudes of the etch rates in these cases are different. Further, the peak values are temperature-dependent.

#### 9.3.2.3 Temperature-dependent etch rates:

Table (9.3) shows the rates of tangential and surface dissolution at various temperatures ranging from 15°C to 50°C for various concentrations of L(+) tartaric acid solutions. Figs.(9.9, 9.10 & 9.11) show the graphs of Log of etch pit widening rate ( $V_{tL}$ ,  $V_{tB}$ ) along directions ( $[110]$ ,  $[\bar{1}\bar{1}0]$ ) and surface dissolution rate ( $V_S$ ) against the reciprocal of temperatures for various concentrations of L(+) tartaric acid. According to Arrhenius equation

$$V = A \exp (-E/KT) \quad \dots \quad \dots \quad (9.1)$$

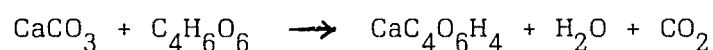
The slope of the graph of Log  $V_{tL}$ , Log  $V_{tB}$  or Log  $V_S$  versus  $1/T$  represents the value of  $E/K$ , where  $E$  is the activation energy of the reacting species and  $K$  is the Boltzmann constant. The straight line graphs are observed for each concentration of the etchant and the activation energies for various concentrations are calculated. The energies thus calculated for all concentrations of L(+) tartaric acid solution are shown in table 9.4. From the table it is clear that the activation energies  $E_{tL}$ ,  $E_{tB}$  and  $E_S$  are different at different etchant concentrations.

#### 9.4 DISCUSSION:

The observations on matching of etch pits produced by an etchant on oppositely matched cleavage counterparts had shown practically complete one-to-one correspondence so far as the location, number and orientation of etch pits were concerned. Further, when a cleavage surface was etched by an etchant (L(+) tartaric acid) and its counterpart by another etchant such as aqueous solution of sodium hydroxide, lactic acid, formic acid, etc., the matching of etch pits on identical areas of these counterparts was fairly good. Successive etching of the same cleaved surface by an etchant had produced the growth of etch pits at unchanged positions on the cleavage surface and that no new pits were formed. Further the etch pits are almost of same sizes. When thin flakes of cleavage plates of calcite (thickness  $\sim 0.01$  mm) were etched, good correspondence of etch pits on the front and reverse faces was also noticed. All these experiments indicate that pits were produced at dislocations terminating on the surface under observation; hence all etchants reveal dislocations. Whether they reveal all dislocations or not is not considered in the present report. Further, while considering the matching of etch pits on cleavage counterparts, it was observed in some cases that flat-bottomed etch pits on one cleavage surface had correspondence with point-bottomed etch pits on its opposite counterpart. This suggests that dislocations at the seat of point-bottomed etch pits had moved during the process of cleaving and/or etching. Hence the flat-bottomed pits are produced at these places. It should be noted that occasionally terraced triangular etch pits were also observed on a cleavage surface. It should also be recorded that as far as the locations of etch pits on oppositely matched cleavage counterparts are concerned, there is almost a perfect matching. However, this is not true for internal structure of etch pits, i.e., the correspondence of etch pit structure on identical areas of cleavage counterparts is sometimes poor. This also suggests that the interactions of specific class of defects, namely, dislocations with the etchant (D-tartaric acid) are different in the

counterparts. The average density of dislocations revealed by etching is  $10^4$  per  $\text{cm}^2$ . This corresponds with the values of dislocation etch pit density obtained by using other etchants.

The basic chemical reaction between calcite and L (+) tartaric acid is as follows:



The product calcium tartrate  $\text{CaC}_4\text{O}_6\text{H}_4$  is soluble in water and hence it does not remain on cleavage surface subjected to etching. L (+) tartaric acid satisfies most of the requirement of a good etchant. They are as follows:

- (a) The etchant is simple in composition and stable so that its concentration will not change appreciably upon standing or during use at room temperature and also at moderately higher or lower temperatures.
- (b) It has constant characteristics at a particular temperature so that the conditions of etching can be easily reproduced. The important conditions are (i) etching time, and (ii) etching temperature. These effects are reported earlier (cf. 9.3.1.1, 9.3.1.3).
- (c) While etching a specimen, L (+) tartaric acid does not form products which precipitate on the specimen surface. The reaction product calcium tartrate immediately dissolves in the solution and has a closer affinity with L (+) tartaric acid than with calcite.
- (d) It is non-injurious and non-toxic to the worker conducting work.

Ideally an etchant should be of such a composition that it will give good all-round results and reveal the greatest number and variety of structural defects, characteristics and irregularities present. At the same time, it should be able to distinguish its

effect from those produced by any of the etchants which can attack only definite type of defects. Thus this selective etching should enable one to study only specific defects. However ideal conditions are not completely realised in practice. Hence it is necessary to discuss several aspects of etching such as quality of etch pits.

#### 9.4.1 Quality of etch pits:

The quality of etch pits includes considerations of the shape, symmetrical nature, contrast of the pits with respect to the surrounding and etch pit size produced on the surface under consideration.

The condition for the formation of visible etch pits on a crystal surface subjected to etching are (i)  $V_n/V_t > 0.1$ , and (ii)  $V_n/V_s > 1/14$ . Later it was reported /17/ that for the formation of visible etch pits, in addition to the above conditions, the ratio of tangential rate of dissolution,  $V_t$ , to that of surface dissolution,  $V_s$ , i.e.,  $V_t/V_s$  should be greater than 10 and higher the ratio ( $V_t/V_s$ ) better is the quality of etch pits. Study of table 9.3 shows that the ratio  $V_t/V_s$  is large. The basic plane shape of etch pit is a triangle. The directions  $[110]$  and  $[\bar{1}\bar{1}0]$  are important on a cleavage plane of calcite. Hence for consideration of quality of etch pits, instead of the ratio  $V_t/V_s$ , the ratios along the directions  $[110]$  and  $[\bar{1}\bar{1}0]$  of tangential dissolution rate to surface dissolution rate, namely,  $V_{tL}/V_s$  and  $V_{tB}/V_s$  should be considered. These values are given in table 9.3. It is clear from the table that the ratios  $V_{tL}/V_s$ ,  $V_{tB}/V_s$  decrease with increase in temperature. Plots of  $V_{tL}/V_s$  versus C and  $V_{tB}/V_s$  versus C indicate initial decrease with increase in concentration attaining minimum values at 0.075 M etchant concentration (for all temperatures). Thereafter they increase with rise of concentration. The minimum values of  $V_{tL}/V_s$  and  $V_{tB}/V_s$  are essentially the maximum rates of tangential and surface dissolution (Fig.9.5 and 9.6). These maximum values will be represented by an additional subscript P, i.e.,  $V_{tLP}$ ,  $V_{tBP}$  and  $V_{sP}$ . Thus the minimum values of these rates will be indicated by  $(V_{tLP}/V_{sP})_{\min}$ ,  $(V_{tBP}/V_{sP})_{\min}$ . These values are independent of etching temperatures.

For a pyramidal etch pit with triangular plane shape on a cleavage surface, the etch rates along [110] and  $[\bar{1}\bar{1}0]$  and their ratios are important, i.e.,  $V_{tLP}$ ,  $V_{tBP}$  and  $V_{tLP}/V_{tBP}$ . These values are shown in table 9.3. It is clear from the table that on an average the value of  $V_{tLP}/V_{tBP}$  is 2 and is almost independent of etching temperature and etchant concentration values mentioned here.

It is thus clear that for considering quality of etch pits, it is not only necessary to consider individual values of  $V_s$ ,  $V_t$  and  $V_n$  but also  $V_{tL}/V_s$  &  $V_{tB}/V_s$ ,  $V_{tLP}/V_{sP}$  and  $V_{tLP}/V_{tBP}$  values and etching temperature. It is necessary to consider in detail the maxima of  $V_{tB} - C$ ,  $V_{tL} - C$  and  $V_s - C$  plots. In addition to these considerations, data on the specific properties of a dislocation etchant, namely, electrolytic conductivity and viscosity of aqueous solution of L(+) tartaric acid will provide information on the mobility and availability of ions taking active part in the etching process. Further it is also interesting to determine how these quantities change with temperature. This data is likely to throw more information about the quality of etch pits.

#### 9.4.2 Maxima in etch rates versus concentration plots:

The nature of  $V - C$  plots ( $V_{tL} - C$ ,  $V_{tB} - C$ ,  $V_s - C$ ,  $V_{tL}/V_s - C$ ,  $V_{tB}/V_s - C$  plots) is illustrated in Figs.9.3 to 9.6. The rate of chemical reaction increases with increase of solute amount in fixed amount of distilled water. It attains maximum value,  $V_{tLP}$ ,  $V_{tBP}$  and  $V_{sP}$  and for higher concentrations it decreases. Sangwal and Patel /9/, Sangwal and Arrora /28/ reported the occurrence of such peaks in their studies on dissolution of MgO crystal cleavages in HCl, HNO<sub>3</sub>, H<sub>2</sub>SO<sub>4</sub> and H<sub>3</sub>PO<sub>4</sub> solutions. The nature of  $V - C$  plots was explained on the basis of adsorption phenomena. The equation of the rate /27-29/ is given by

$$V = \frac{KC_a}{1 + K_a C_a} \quad \dots \quad \dots \quad (9.1)$$

for moderate adsorption of the reactant and weak adsorption of reaction products where  $K$ ,  $K_a$  are constants and  $C_a$  is the acid concentration. It was claimed that equation (9.1) explains the nature of plots. If equation (9.1) explains the nature of  $V - C$  plots, then mathematically the condition for obtaining extremum, viz.,

$$\left( \frac{dV}{dC_a} \right)_{C_a = 0} = 0 \quad \text{must be satisfied.}$$

Now differentiating equation (9.1) with respect to  $C_a$  yields,

$$\left( \frac{dV}{dC_a} \right) = \frac{K}{(1 + K_a C_a)^2}$$

and for an extremum,

$$\left( \frac{dV}{dC_a} \right) = 0 = \frac{K}{(1 + K_a C_a)^2}$$

This implies that  $K$  must be zero or  $C_a$  must be infinite. None is possible in view of the finite value of  $V$  (equation 9.1). Thus equation (9.1) is not able to explain the nature of  $V - C$  plots.

There are several factors which appear to be responsible for the general characteristics of  $V - C$  plots, namely, etching rate increases with etching temperature, the increase is non-linear in nature, the rate has a maximum value for a given temperature. The maximum value increases with etching temperature, for all etching temperatures, the maximum value of etchant concentration is  $C_p$  (or within a small concentration range around  $C_p$ ), it then falls to a lower value in a non-linear manner. These factors are as follows:

- (1) Availability of ions in the etchant,
- (2) Ionic conductivity of the etchant,

- (3) Viscosity of the etchant,
- (4) Inhibition of reaction products,
- (5) Chemical nature of crystal and arrangement of atoms on the cleavage surface.

The increase of reaction rate ( $V_t$  or  $V_s$ ) with increase of etchant concentration may be due to increase of ions reacting with crystal surface. With increase of solute in fixed amount of solvent (distilled water) the reactivity of the etchant increases. This may be responsible for increase of rates. As mentioned earlier, instead of  $V_t$ , it is necessary to consider  $V_{tL}$  and  $V_{tB}$  along directions  $[110]$  and  $[\bar{1}\bar{1}0]$  with respect to  $V_s$ , i.e., ratios  $V_{tL}/V_s$  and  $V_{tB}/V_s$  are to be considered for the development of edges along these directions. Decrease of  $V_{tL}/V_s$  and  $V_{tB}/V_s$  with increase in concentration at constant etching temperature does not indicate that  $V_s$  is more than  $V_{tL}$  and  $V_{tB}$ , it simply indicates a relative change (decrease) of ratio ( $V_{tL}/V_s$ ) and ( $V_{tB}/V_s$ ) with increase of concentration. This trend continues upto a value  $C_p$  of etchant concentration where the ratios ( $V_{tL}/V_s$ ) and ( $V_{tB}/V_s$ ) have minimum values. With values of concentration beyond  $C_p$ , there is a relative increase of ratio ( $V_{tL}/V_s$  &  $V_{tB}/V_s$ ). For the minimum values of ratios, the individual values of rates  $V_{tL}$ ,  $V_{tB}$  and  $V_s$  correspond to peak values in the plots of  $V_{tL}$  Vs.  $C$ ,  $V_{tB}$  Vs.  $C$  and  $V_s$  Vs.  $C$ . These values are indicated by  $V_{tLP}$ ,  $V_{tBP}$  &  $V_{sP}$  and minimum values of ratios by  $(V_{tLP}/V_{sP})_{\min}$ ,  $(V_{tBP}/V_{sP})_{\min}$ . It should be noted that around  $C_p$  where the minimum values of ratios are observed, the triangular etch pits are bound by sharp edges (Table 9.1). It is also interesting to note that after a certain etchant concentration on either side of  $C_p$  the plane shape of etch pit is a curvilinear triangle. It is thus clear from the above discussion that for considering quality of etch pit, individual peak values of  $V_{tL} - C$ ,  $V_{tB} - C$  and  $V_s - C$  are not to be considered but their ratios  $V_{tLP}/V_{sP}$  and  $V_{tBP}/V_{sP}$  are to be considered at this etchant concentration value ( $C_p$ ).

### 9.4.3 Reaction product inhibition:

The inhibition of reaction products is a possible factor for decrease of etch rates at concentrations greater than  $C_p$ . The dependence of reaction of etching time (t) for weak and strong adsorption of reaction products on a crystal surface is given by,

$$\delta_w = K_1 t \quad \dots \quad (9.2)$$

$$\delta_s = K_2 t \quad \dots \quad (9.3)$$

where  $\delta$  is desorption rate; suffixes w and s indicate desorption to be weak and strong respectively.  $K_1$  and  $K_2$  are constants. If the adsorption of reaction products is weak, the plot of reaction versus time should be a straight line (cf. eqn. 9.1). In the present work, the graphs (Fig.9.1 and 9.2) of Length and Breadth of an etch pit along directions [110] &  $[\bar{1}\bar{1}0]$  and weight loss per  $\text{cm}^2$  against etching time are straight lines. Hence adsorption of reaction products is weak in dissolution of calcite in aqueous solutions of L(+) tartaric acid. For strong adsorption, the plot of reaction versus etching time should be a parabola, which is not found to be the case for the range of etchant concentrations and etching times and temperatures studied in the present investigation. Thus the reaction product does not inhibit the chemical reaction rate, i.e.,  $V_s$ . This can be seen from the fact that after etchant concentration 0.075 M,  $V_{tL}$ ,  $V_{tB}$ ,  $V_s$  decrease and  $V_{tL}/V_s$ ,  $V_{tB}/V_s$  increase from their values  $V_{tLP}/V_s$ ,  $V_{tBP}/V_{sP}$  (table 9.2), thereby showing dissolution of greater number of surface layers and less dissolution at preferential points. The etching temperature is also an important parameter in the etching process. This can be realised from a study of Arrhenius plots. However, if the effects of  $V_t$  and  $V_s$  are independently considered, the reaction product does inhibit the chemical reaction after a concentration of 0.075 M L(+) tartaric acid. Since the effects of tangential and surface dissolution are jointly considered, the inhibition effect due to separate  $V_t$  and  $V_s$  can not be considered.

#### 9.4.4 Importance of activation energy:

Surface dissolution by most of the etchants producing etch pits is independent of line defects. The surface dissolution has been attributed /30,31/ to the presence of other short-lived defects such as lattice impurities. It plays an important role in the etching process. The plane shape of a pyramidal/flat bottomed/terraced etch pits on a calcite cleavage depends on etchant concentration /19,21/ and etching temperature. For a definite concentration of the etchant (acetic acid) /20/ and for temperatures within a given temperature range, plane shape of an etch pit is invariant within the limits of optical resolution. The activation energy was found to be constant /20/. The changes in activation energy were also noticed with gradual changes in range of temperature. The very fact that the strong alkaline etchant (aqueous NaOH solution) does not show noticeable change of shape for various temperatures and concentrations indicates that plane shape depends also on the nature of the etchant and possibly a crystal surface under attack. The present work indicates that the plane shape of etch pits produced by L(+) tartaric acid is not affected by range of etchant concentrations studied. The values of activation energies and  $E_{tL}$ ,  $E_{tB}$  and  $E_s$  for various etchant concentrations had disclosed a surprising fact: although plane shape of etch pit is invariant, the activation energy depends on etchant concentration and is different for different concentrations and that the energies for dissolution of ledges along  $[110]$  and  $[\bar{1}\bar{1}0]$  directions are also different indicating the anisotropy of etch rates. This should be compared with the chemical etching studies of calcite cleavages subjected to aqueous solution of acetic acid (0.078 M) and hydrochloric acid (0.0275 M) /20/. Lactic acid (0.111 M) /18/ and ammonium chloride (9 M). All these etchants produce rhombic shapes for which the activation energies are 0.68, 0.02, 0.99 and 0.35 eV respectively. This indicates that for identical shapes of etch pits on calcite cleavages the activation energies for different etchants are different. Similarly activation energies for boat-shaped etch pits produced by different concentrations of aqueous solutions of NaOH and lactic acid (1.64 M) are 0.62 and 0.20 eV,

respectively. Thus it can be safely generalized that for a given crystal face and plane shape of etch pits, activation energies are etchant-dependent. This also suggests that attack on a crystal surface is a characteristic of an etchant and not of the surface.

A glance at table 9.4 indicates that the activation energies for tangential dissolution rates along  $[110]$  &  $[\bar{1}\bar{1}0]$ , and for surface dissolution rates, viz.,  $E_{tL}$ ,  $E_{tB}$  and  $E_s$  are different.  $E_{tL}$  is greater than  $E_{tB}$  whereas  $E_s$  has the greatest value for an etchant concentration. From the analysis of  $V - C$  plots it is clear that it is the joint effects of  $V_{tL}$ ,  $V_{tB}$  and  $V_s$  and not the individual effects which control the quality of etch pits. Just as the ratios  $V_{tLP}/V_{sP}$ ,  $V_{tBP}/V_{sP}$  and  $V_{tLP}/V_{tBP}$  are considered for obtaining the above conclusion, it is necessary to consider the ratios of the activation energies, namely  $E_{tL}/E_s$ ,  $E_{tB}/E_s$  and  $E_{tL}/E_{tB}$ . These are shown in table 9.4. It is clear from the values of these ratios at  $C_p$  (= 0.075 M) that  $E_{tL}$  &  $E_{tB}$  differ by a very small amount and that they can be considered almost identical at  $C_p$ . This is not true for any other etchant concentration. It is also clear from the table that although the difference  $E_s - E_{tL}$  and  $E_s - E_{tB}$  is relatively large and positive for various etchant concentrations it is very small and positive at  $C_p$ . This indicates that at  $C_p$ ,  $E_s$  is slightly greater than  $E_{tL}$  &  $E_{tB}$  and that  $E_{tL}$  &  $E_{tB}$  differ by a very small amount. This leads to the conclusion that for etchant concentration  $C_p$  at the temperature-dependent maxima of  $V - C$  ( $V_{tL}$  versus  $C$ ,  $V_{tB}$  versus  $C$ ,  $V_s$  versus  $C$ ) plots or temperature-dependent minima of  $(V_{tLP}/V_{sP})$  versus  $C$  and  $(V_{tBP}/V_{sP})$  versus  $C$  plots, the activation energies  $E_{tL}$  and  $E_{tB}$  are approximately equal and that  $E_s$  is slightly greater than  $E_{tL}$  or  $E_{tB}$ . For these conditions, the quality of etch pit is superior (photomicrograph in table 9.1). In view of this conclusion, it is desirable to determine the variation of Electrolytic Conductivity of etchant with concentration and temperature.

#### 9.4.5 Electrolytic conductivity of etchant:

In view of the above analysis of the occurrence of maxima in the  $V - C$  plots, and importance of activation energies for a chemical process, it is necessary to determine the availability and mobility of ions at the etchant concentration  $C_p$ . The etchant is an electrolyte and electrical conductivity of electrolyte of different concentrations and at different temperatures was determined. The values of temperatures and etchant (electrolyte) concentrations are those which were used earlier. The plots of  $\sigma$  Vs.  $C$  for various temperatures of electrolytes are straight lines as shown in Fig.(9.7). It is clear from these plots that at concentration  $C_p$  there is a slight spur or kink indicating a change in the slope of the straight line plot. This indicates the existence of two straight lines (two regions) in the  $\sigma$  Vs.  $C$  plots, the point separating these regions is given by  $C_p$ ,  $\sigma_p$ . This point depends on temperature. The values of  $\sigma_p$ , electrolyte temperature, slopes of these two straight lines  $S_1$  &  $S_2$  and their ratio  $S_1/S_2$  are shown below.

$\sigma_p$ milli-mho-cm <sup>-1</sup>	T° K	Slope of first line before kink $S_1 \times 10^{-3}$	Slope of second line after kink $S_2 \times 10^{-3}$	$\frac{S_2}{S_1}$
2.216	288	18.0	11.2	1.6071
2.8	298	26.0	17.6	1.477
3.083	303	23.0	16.0	1.437
3.546	313	32.0	15.2	2.105
3.94	323	36.0	16.0	2.25

The detail values of  $\sigma$  for different concentrations and temperatures are given in table (9.5).

The electrolytic conductivity is given by-

$$\sigma = nS\mu_s$$

where,  $n$  = concentration of charge carriers.

$S$  = carrier charge

$\mu_s$  = carrier mobility

Since  $S$  has a constant value,

$$n\mu_s = \frac{\sigma}{S}$$

represents the product of mobility and concentration of charge carriers.

The slope of the straight line plot of  $\sigma$  Vs.  $C$  is given by-

$$\frac{\Delta\sigma}{\Delta C}$$

where  $\Delta\sigma$  is the difference between two neighbouring points differing by a concentration  $\Delta C$ . Thus,

$$\frac{\Delta\sigma}{\Delta C} = \text{Slope} = \frac{\Delta(nS\mu_s)}{\Delta C}$$

$$\frac{\Delta(n\mu_s)}{\Delta C} = \frac{\text{Slope}}{S}$$

Since the slopes  $S_1$  &  $S_2$  of the two straight lines are given above, their ratios ( $S_2/S_1$ ) represent change in  $n\mu_s$  per unit concentration change. Since  $n$  and  $\mu_s$  can not be separated, it is not possible to present a comparative study of the individual effects of carrier-concentration and mobility and their combined effects on the quality of etch pits.

The plots of  $\log \sigma$  Vs.  $10^3/T$  are shown in Fig. (9.12). For concentration values ranging from 0.025 M to 0.2 M, the slopes are

different, giving rise to activation energy values as a function of concentration. It is also interesting to observe that near about  $C = 0.175$  M concentration, the scattering of points around the straight line plot is more; the scattering of the conductivity values at  $288^\circ\text{K}$  ( $15^\circ\text{C}$ ) is more noticeable. It is difficult to appreciate this noticeable deviation from the straight line plot. It simply indicates that the mobility and availability of number of ions, represented by the product  $n \mu_s$  ( $= \sigma/S$ ) are unusually different from the ones found for different etchant concentrations. A careful study of the activation energies of ions in the etchant indicates that near about  $C_p$  ( $0.075$  M) they are more active and thereafter activity noticeably decreases. Qualitatively this means that either the ions are more active by having a group effect or their mobility is more. Study of viscosity data of the etchant at various concentrations and temperatures is likely to suggest the relative importance of  $n$  and  $\mu_s$ .

#### 9.4.6 Viscosity of Etchant:

Etchant viscosity ( $\mu$ ) is determined for various etchant concentrations and at different etching temperatures and is presented in table 9.6. From these values, a graph of  $\log \mu$  Vs.  $10^3/T$  is drawn. A surprising fact emerges: for all values of etchant concentrations, there is a single straight line. This suggests that the part played by etchant viscosity in the chemical etching of calcite cleavages by aqueous solution of L(+) tartaric acid is not significant. Further, in this case activation energy of the etchant is found to be  $0.165$  eV (Fig.9.8). A comparison of the activation energies for a chemical reaction between calcite cleavages and the etchant, the activation energy for the electrolytic process in the etchant with the one obtainable from viscosity studies shows very clearly that although  $E_\mu$  is greater than  $E_t$ ,  $E_s$  and  $E_\sigma$  it does not appear to play a significant role in the etch phenomena on calcite cleavages. With the data available on the activation energies from chemical etching, electrolytic conductivity and viscosity of etchant, it is

possible to conjecture the mechanism of chemical dissolution of cleavage faces of calcite.

#### 9.4.7 Mechanism of Dissolution:

Any catalytic reaction proceeds in the following steps /28/:

- (1) diffusion of reacting species,
- (ii) adsorption on the surfaces,
- (iii) reaction on the surface,
- (iv) desorption of reaction products, and
- (v) diffusion of products away from the surface.

Depending upon the condition in which the process is conducted, a reaction can be diffusion controlled or kinetically controlled. The rate of diffusion changes with temperature according to the law similar to the Arrhenius equation /29/,

$$D = K \exp(-E/RT) \quad \dots \quad (9.4)$$

where,

- D = diffusion rate,
- K = constant having same dimension as that of D,
- E = activation energy for diffusion process,
- R = universal gas constant,
- T = temperature in °K.

It should be noted that the value of E rarely exceeds 1000 - 2000 calories per mole (0.05 - 0.10 eV), i.e., it is only a fraction of the activation energies of most of the reactions. Consequently the rate of diffusion will increase with temperature considerably slower than the rate of chemical reaction. Viscosity and diffusion are correlated /32/. From the plot of  $\log \mu$  Vs.  $10^3/T$  (Fig.9.8), activation energy  $E_{\mu}$  is determined. For liquids which have low viscosity at room temperature, the value of activation energy  $E_{\mu}$

is usually 0.14 eV. For denser solution two values are reported /27/. If  $E_{\mu}$  and activation energy of dissolution  $E_s$  happen to be approximately equal, the dissolution kinetics are fully diffusion controlled /9,33/. Further, the activation energy for a diffusion controlled mechanism is usually less than that of kinetically controlled one /34/. In the present case  $E_{tL}$  &  $E_{tB}$  are less than  $E_{\mu}$  and  $E_{\mu}$  is less than  $E_s$ . The values of  $E_s/E_{\mu}$  for various etchant concentrations are given below:

Etchant Concentration in M	0.025	0.05	0.075	0.1	0.125	0.15	0.175	0.2
$E_s/E_{\mu}$	1.363	1.424	1.09	1.2	1.2	1.139	0.975	0.957

It is clear from the above table that for low concentrations  $E_s$  is greater than  $E_{\mu}$  and at  $C_p = 0.075$ ,  $E_s$  is approximately equal to  $E_{\mu}$ . Hence it can be guessed that the dissolution kinetics are fully diffusion controlled. This conjecture is supported by the straight line plots of etch pit length and breadth along [110] and  $[\bar{1}\bar{1}0]$  and weight loss per  $\text{cm}^2$  Vs. etching time, giving constant values of etch rates at a constant etching temperature and indicating weak adsorption of reaction products.

#### 9.5 CONCLUSIONS:

- (1) Plane shape of an etch pit produced by different concentrations of L(+) tartaric acid solution on cleavage face of calcite is independent of etchant concentrations. The pits near the highest concentration exhibit sharp beak; however the shape is not changed.

- (2) Etch rates are independent of etching time but depends on etchant concentration and etchant temperature.
- (3) The  $C_p$  value of the etchant is independent of etching temperature.
- (4) Beyond  $C_p$  the etch rates decrease with increase of etchant concentration.
- (5) In the study of etch phenomena, the ratio  $V_{tP}/V_{sP}$  (i.e.,  $V_{tLP}/V_{sP}$ ,  $V_{tBP}/V_{sP}$ ) and  $V_{tLP}/V_{tBP}$  should be considered. For all dislocation etchants the relation between  $V_{tP}/V_{sP}$  and concentration  $C$  and also between  $O_p$  and  $C$  are linear and independent of etching temperature.
- (6) For the triangular etch pits the ratio  $V_{tL}/V_{tB}$  is 2 and constant for all etching temperatures and etchant concentrations.
- (7) A careful study of the activation energies of ions indicates that near about  $C_p$  (0.075 M) they are more active and thereafter activity noticeably decreases. Qualitatively this means that either the ions are more active by having a group effect or their mobility is more.
- (8) For etchant concentration  $C_p$  at the temperature dependent maxima of  $V - C$  plots ( $V_{tL}$  Vs.  $C$ ,  $V_{tB}$  Vs.  $C$ ,  $V_s$  Vs.  $C$ ) or at temperature dependent minima of  $(V_{tLP}/V_{sP})$  Vs.  $C$  and  $(V_{tBP}/V_{sP})$  Vs.  $C$  plots, the activation energies  $E_{tL}$  and  $E_{tB}$  are approximately equal and that  $E_s$  is slightly greater than  $E_{tL}$  or  $E_{tB}$ . For these conditions, the quality of etch pit is superior.
- (9) Although  $E_\mu$  is greater than  $E_t$ ,  $E_s$  and  $E_\sigma$ , it does not appear to play a significant role in the etch phenomena on calcite cleavages.
- (10) The chemical dislocation of calcite in L(+) tartaric acid with concentration  $C_p$  is diffusion controlled, at  $C_p$ .

TABLE - 9.1

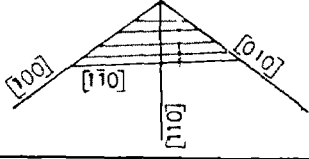
Percussion figure		Etchant: L(+)-Tartaric Acid Etchant Temp: 50°C Orientation of each pit with respect to percussion star all parallel
Concentration in M	Etch pit shape	
0.025	△	
0.05	△	
0.075	△	
0.1	△	
0.125	△	
0.15	△	
0.175	△	
0.2	△	
Photomicrograph of an etch pit for concentration 0.075 M and temp 50°C		

TABLE 9.2

Concentration: C = 0.075 M, Temperature = 15°C			
Etching time t in sec.	Length L of an etchpit x 10 <sup>-4</sup> cm	Breadth B of an etchpit x 10 <sup>-4</sup> cm	Wt. loss/Area in gm/cm <sup>2</sup> x 10 <sup>-5</sup>
10	5.50	6.50	6.50
20	14.43	11.55	13.68
30	25.50	16.50	21.05
40	35.47	20.60	28.50
50	45.50	26.00	36.00
Concentration: C = 0.075 M, Temperature = 25°C			
10	12.70	6.18	8.21
20	23.50	11.90	17.30
30	33.80	17.30	25.52
40	44.50	22.60	34.61
50	55.60	28.40	43.68
Concentration: C = 0.075 M, Temperature = 30°C			
10	14.02	10.73	12.70
20	26.40	16.90	23.95
30	39.60	22.68	34.73
40	50.32	28.46	46.01
50	61.05	34.65	57.07
Concentration: C = 0.075 M, Temperature = 40°C			
10	16.50	9.90	13.49
20	30.52	18.15	26.99
30	45.78	26.81	41.45
40	59.40	34.65	54.47
50	73.83	42.90	67.01
Concentration: C = 0.075 M, Temperature = 50°C			
10	16.09	9.07	16.91
20	35.88	18.15	33.81
30	56.11	27.22	51.01
40	75.91	35.88	67.91
50	95.28	44.55	83.98

TABLE 9.3 (A)

Part I

(i) Concentration C = 0.025 M						
Temp T°K	$V_{tL}$ in cm/sec $\times 10^{-4}$	$V_{tB}$ in cm/sec $\times 10^{-4}$	$V_s$ in cm/sec $\times 10^{-6}$	$\frac{V_{tL}}{V_s}$	$\frac{V_{tB}}{V_s}$	
288	0.8	0.41	1.15	69.56	35.65	
298	0.8	0.425	1.47	54.42	28.91	
303	0.875	0.425	1.66	52.71	25.60	
313	1.0	0.45	2.49	40.16	18.07	
323	1.2	0.5	3.22	37.26	15.52	
(ii) Concentration C = 0.05 M						
288	0.85	0.425	1.52	55.92	27.96	
298	0.9	0.475	1.93	46.63	24.61	
303	0.925	0.5	2.306	40.11	21.68	
313	1.25	0.625	3.5	35.71	17.85	
323	1.475	0.725	4.33	34.06	16.74	
(iii) Concentration C = 0.075 M						
288	1.0	0.45	2.58	38.75	17.44	
298	1.075	0.525	3.22	33.38	16.30	
303	1.175	0.6	3.874	30.33	15.48	
313	1.425	0.825	4.98	28.61	16.56	
323	2.0	0.875	6.36	31.44	13.75	
(iv) Concentration C = 0.1 M						
288	0.95	0.475	2.12	44.81	22.40	
298	0.975	0.5	2.49	39.16	20.08	
303	1.025	0.55	3.044	33.67	18.06	
313	1.375	0.675	3.87	35.52	17.44	
323	1.75	0.7	5.25	33.33	13.33	

Table 9.3 (A)

Part II

(v) Concentration C = 0.125 M					
Temp	$V_{tL}$ in	$V_{tB}$ in	$V_s$ in	$\frac{V_{tL}}{V_s}$	$\frac{V_{tB}}{V_s}$
T°K	cm/secx10 <sup>-4</sup>	cm/secx10 <sup>-4</sup>	cm/secx10 <sup>-6</sup>		
288	0.91	0.425	1.7	53.52	24.28
298	0.975	0.425	2.21	44.11	19.23
303	1.0	0.475	2.49	40.16	19.07
313	1.3	0.575	2.04	42.76	18.91
323	1.45	0.7	4.33	33.48	16.16
(vi) Concentration C = 0.15 M					
288	0.875	0.387	1.66	52.71	23.31
298	0.925	0.425	1.93	47.92	22.02
303	0.975	0.45	2.22	43.92	20.27
313	1.2	0.5	2.58	46.51	19.37
323	1.35	0.55	3.87	34.88	14.21
(vii) Concentration C = 0.175 M					
288	0.837	0.362	1.6	52.31	22.62
298	0.9	0.4	1.84	48.91	21.73
303	0.95	0.425	2.02	47.02	21.03
313	1.1	0.45	2.49	44.17	18.07
323	1.21	0.5	3.41	35.48	14.66
(viii) Concentration C = 0.2 M					
288	0.837	0.35	1.52	55.06	23.02
298	0.875	0.4	1.75	50.0	22.85
303	0.9	0.4	2.029	44.36	19.71
313	1.075	0.45	2.49	43.17	18.07
323	1.1	0.46	3.04	36.18	15.13

TABLE 9.3 (B)

$\frac{V_{tL}}{V_{tB}}$  at various etching temperatures and  
etchant concentrations

C in M	$(V_{tL}/V_{tB})$					Average $(V_{tL}/V_{tB})$
	288°K	298°K	303°K	312°K	323°K	
0.025	1.95	1.88	2.06	2.22	2.4	2.10
0.05	2.0	1.89	1.85	2.0	2.03	1.95
0.075	2.22	2.04	1.95	1.72	2.28	2.04
0.1	2.0	1.95	1.86	2.03	2.5	2.06
0.125	2.14	2.29	2.10	2.26	2.07	2.17
0.15	2.26	2.17	2.16	2.4	2.45	2.28
0.175	2.31	2.25	2.23	2.44	2.42	2.33
0.2	2.39	2.18	2.25	2.38	2.39	2.31
Average $V_{tL}/V_{tB}$ For T = Const.	2.15	2.08	2.05	2.18	2.25	2.14

The average ratio  $\frac{V_{tL}}{V_{tB}}$  is constant = 2

It is independent of etchant concentration and etching temperature.

The percentage deviation from 2 is 7%.

TABLE 9.3 (C)

Part I

(i) Concentration C = 0.025 M				
$\frac{10^3}{T}$	Log $V_{tL}$	Log $V_{tB}$	Log $V_S$	Log $\sigma$
3.472	5.9030	5.6127	6.0606	3.1264
3.355	5.9030	5.6283	6.1673	3.1903
3.300	5.9420	5.6283	6.2201	3.2487
3.194	4.0000	5.6532	6.3961	3.3066
3.095	4.0791	5.6989	6.5078	3.3180
(ii) Concentration C = 0.05 M				
3.472	5.9294	5.6283	6.1818	3.282
3.355	5.9542	5.6766	6.2855	3.352
3.300	5.9661	5.6989	6.3628	3.4034
3.194	4.0969	5.7958	6.5441	3.4356
3.095	4.1687	5.8603	6.6364	3.4356
(iii) Concentration C = 0.075 M				
3.472	4.0000	5.6532	6.4116	3.3455
3.355	4.0314	5.7201	6.5078	3.4471
3.300	4.0700	5.7781	6.5881	3.4889
3.194	4.1538	5.9164	6.6972	3.5497
3.095	4.3010	5.9420	6.8034	3.5954
(iv) Concentration C = 0.1 M				
3.472	5.97777	5.6766	6.3263	3.4192
3.355	5.9890	5.6989	6.3961	3.5118
3.300	4.0107	5.7403	6.4834	3.5607
3.194	4.1383	5.8293	6.5877	3.5954
3.095	4.2430	5.8450	6.7202	3.6201

Table 9.3 (C) (Contd.)

Part II

(v) Concentration C = 0.125 M				
$\frac{10^3}{T}$	Log $V_{tL}$	Log $V_{tB}$	Log $V_s$	Log $\phi$
3.472	5.9590	5.6283	6.2304	3.4527
3.355	5.9890	5.6283	6.3443	3.5622
3.300	4.0000	5.6766	6.3961	3.6076
3.194	4.1139	5.7596	6.4828	3.6434
3.095	4.1613	5.8450	6.6364	3.6746
(vi) Concentration C = 0.15 M				
3.472	5.9420	5.5877	6.2201	3.4889
3.355	5.9661	5.6283	6.2855	3.6074
3.300	5.9890	5.6532	6.3464	3.6465
3.194	4.0791	5.6989	6.4116	3.7045
3.095	4.1303	5.7403	6.5877	3.7367
(vii) Concentration C = 0.175 M				
3.472	5.9227	5.5587	6.2041	3.5285
3.355	5.9542	5.6020	6.2648	3.6721
3.300	5.9777	5.6283	6.3054	3.6746
3.194	4.0413	5.6532	6.3961	3.7204
3.095	4.0827	5.6989	6.5327	3.7367
(viii) Concentration C = 0.2 M				
3.472	5.9227	5.5441	6.1818	3.5497
3.355	5.9420	5.6020	6.2430	3.6989
3.300	5.9542	5.6020	6.3072	3.7045
3.194	4.0314	5.6532	6.3961	3.7367
3.095	4.0413	5.6627	6.4828	3.7715

TABLE 9.3 (D)

Temp T°K	Temp $\frac{1}{T}$ °K <sup>-1</sup> x10 <sup>-3</sup>	Concentration C in M									
		0.025	0.05	0.075	0.1	0.125	0.15	0.175	0.2	log $\mu$ of absolute viscosity -----	
283	3.533	0.1267	0.1225	0.1290	0.1344	0.1652	0.1565	0.1562	0.1519		
288	3.472	0.0737	0.0666	0.0707	0.0820	0.1038	0.0909	0.0986	0.0916		
293	3.413	0.0153	0.0182	0.0236	0.0289	0.044	0.0281	0.0449	0.0322		
298	3.356	1.9718	1.9684	1.9731	1.9827	0.0004	1.9858	1.9894	1.9836		
303	3.300	1.9216	1.9268	1.9375	1.9309	1.9547	1.9469	1.9518	1.9400		
308	3.246	1.8686	1.8744	1.8921	1.8813	1.9036	1.8893	1.8981	1.8954		
313	3.195	1.8188	1.8208	1.8388	1.8388	1.8494	1.8369	1.8432	1.8432		
318	3.144	1.7916	1.7923	1.8061	1.8007	1.7795	1.8041	1.8122	1.8055		
323	3.095	1.7474	1.7442	1.7678	1.7581	1.7693	1.7551	1.7671	1.7596		
328	3.048	1.7084	1.7092	1.7315	1.7242	1.7315	1.7259	1.7267	1.7209		
333	3.003	1.6766	1.6794	1.7015	1.6893	1.7050	1.6910	1.6981	1.6901		
338	2.958	1.6512	1.6483	1.6473	1.6618	1.6766	1.6646	1.6711	1.6646		
343	2.915	1.6146	1.6170	1.6374	1.6304	1.6364	1.6253	1.6364	1.6273		
348	2.873	1.5854	1.5831	1.6020	1.5921	1.6042	1.5943	1.6053	1.5943		
353	2.832	1.5797	1.5831	1.5693	1.5670	1.5786	1.5921	1.5465	1.5693		



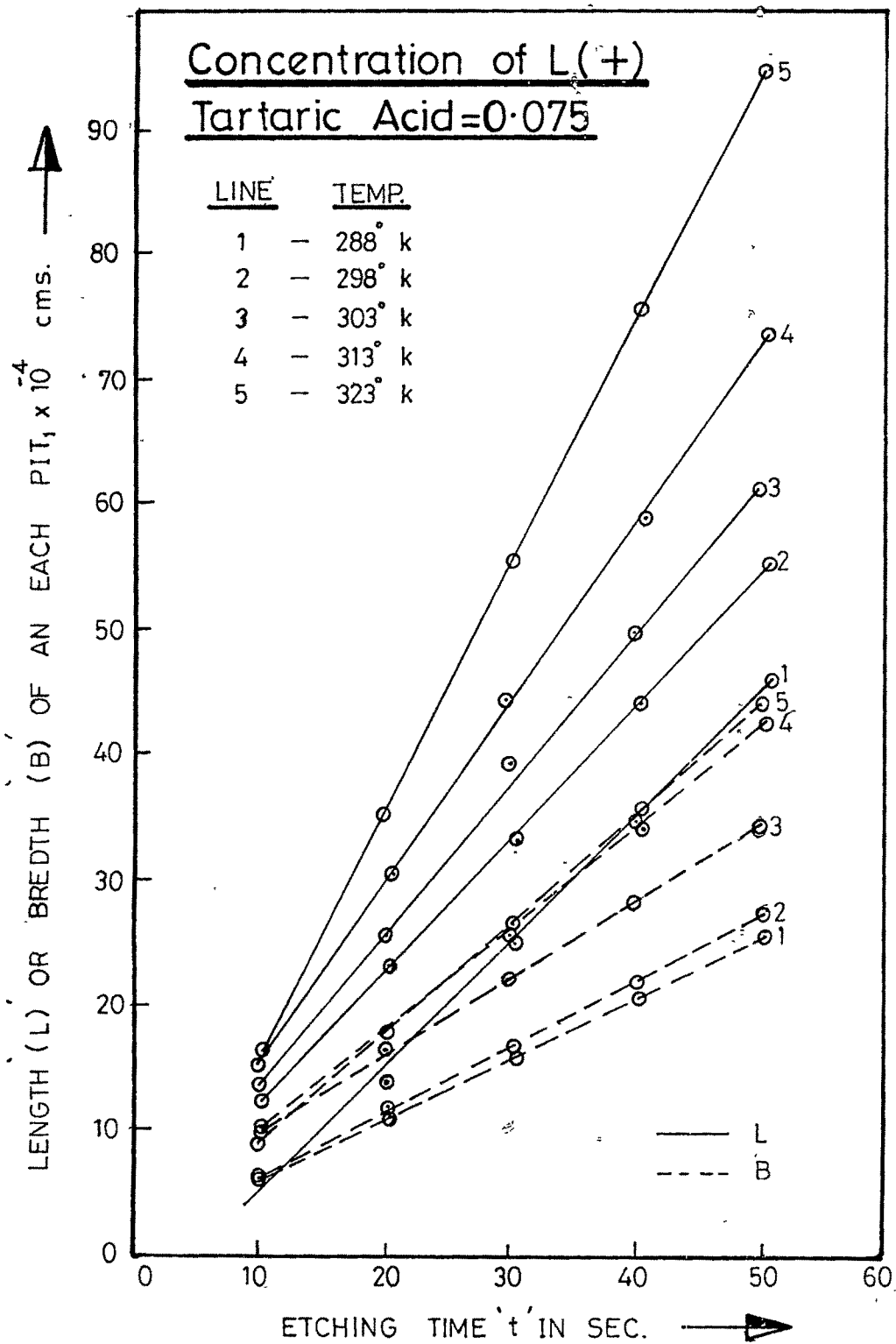
TABLE 9.5

Temp t°C	Temp T°C	Sp. Conductivity $\sigma$ of liquid in $\mu\sigma/\text{cm} \times 10^3$ or milli $\sigma/\text{cm}$							
		0.025M	0.05M	0.075M	0.1M	0.125M	0.15M	0.175M	0.2M
15	288	1.338	1.916	2.216	2.626	2.836	3.083	3.377	3.546
25	298	1.55	2.25	2.8	3.25	3.65	4.05	4.7	5.0
30	303	1.773	2.532	3.083	3.637	4.052	4.432	4.728	5.065
40	323	2.08	2.727	3.546	3.94	4.4	5.065	5.253	5.455
50	323	2.08	2.727	3.94	4.17	4.728	5.455	5.455	5.91

TABLE 9.6

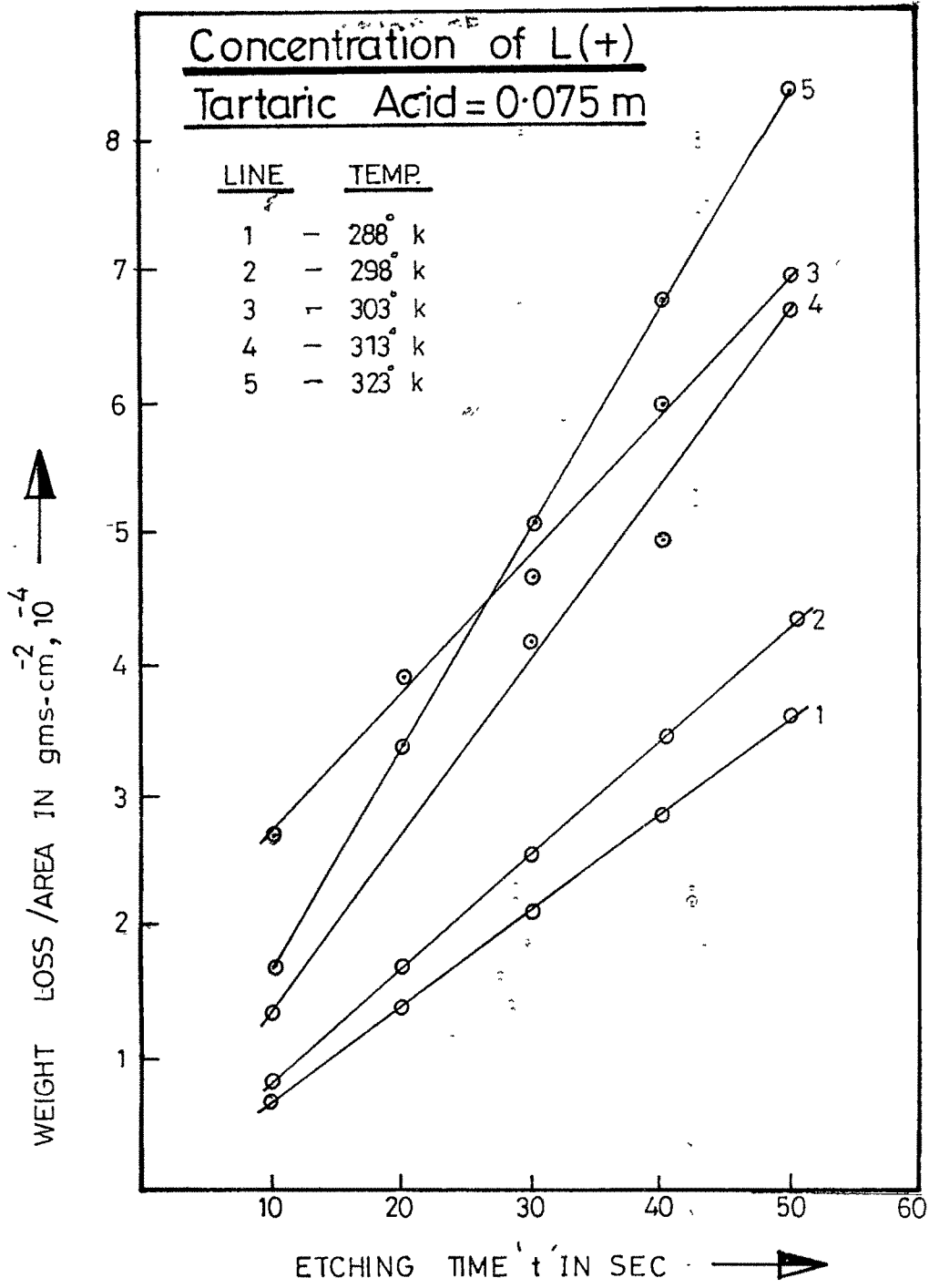
Absolute viscosity  $\mu$  in cp

Concentration		Absolute viscosity $\mu$ in cp									
Temp t°C	C in M	0.025	0.05	0.075	0.1	0.125	0.15	0.175	0.2		
	10	1.339	1.326	1.346	1.363	1.463	1.434	1.433	1.419		
	15	1.185	1.166	1.177	1.208	1.270	1.233	1.255	1.235		
	20	1.036	1.043	1.056	1.069	1.107	1.067	1.109	1.077		
	25	0.937	0.930	0.940	0.961	1.001	0.968	0.976	0.963		
	30	0.835	0.845	0.866	0.853	0.901	0.885	0.895	0.871		
	35	0.739	0.749	0.780	0.761	0.801	0.775	0.791	0.786		
	40	0.659	0.662	0.690	0.690	0.707	0.687	0.697	0.697		
	45	0.619	0.620	0.640	0.632	0.602	0.637	0.649	0.639		
	50	0.559	0.555	0.586	0.573	0.588	0.569	0.595	0.575		
	55	0.511	0.512	0.539	0.530	0.539	0.532	0.533	0.526		
	60	0.475	0.478	0.503	0.489	0.507	0.491	0.499	0.490		
	65	0.448	0.445	0.444	0.459	0.475	0.462	0.469	0.462		
	70	0.412	0.414	0.434	0.427	0.433	0.422	0.433	0.424		
	75	0.385	0.383	0.400	0.391	0.402	0.393	0.403	0.393		
	80	0.360	0.383	0.371	0.369	0.379	0.391	0.352	0.371		



Plot of 'L or B' vs 't'

Fig. : 9.1



Plot of Loss / Area vs Etching Time

Fig. : 9.2

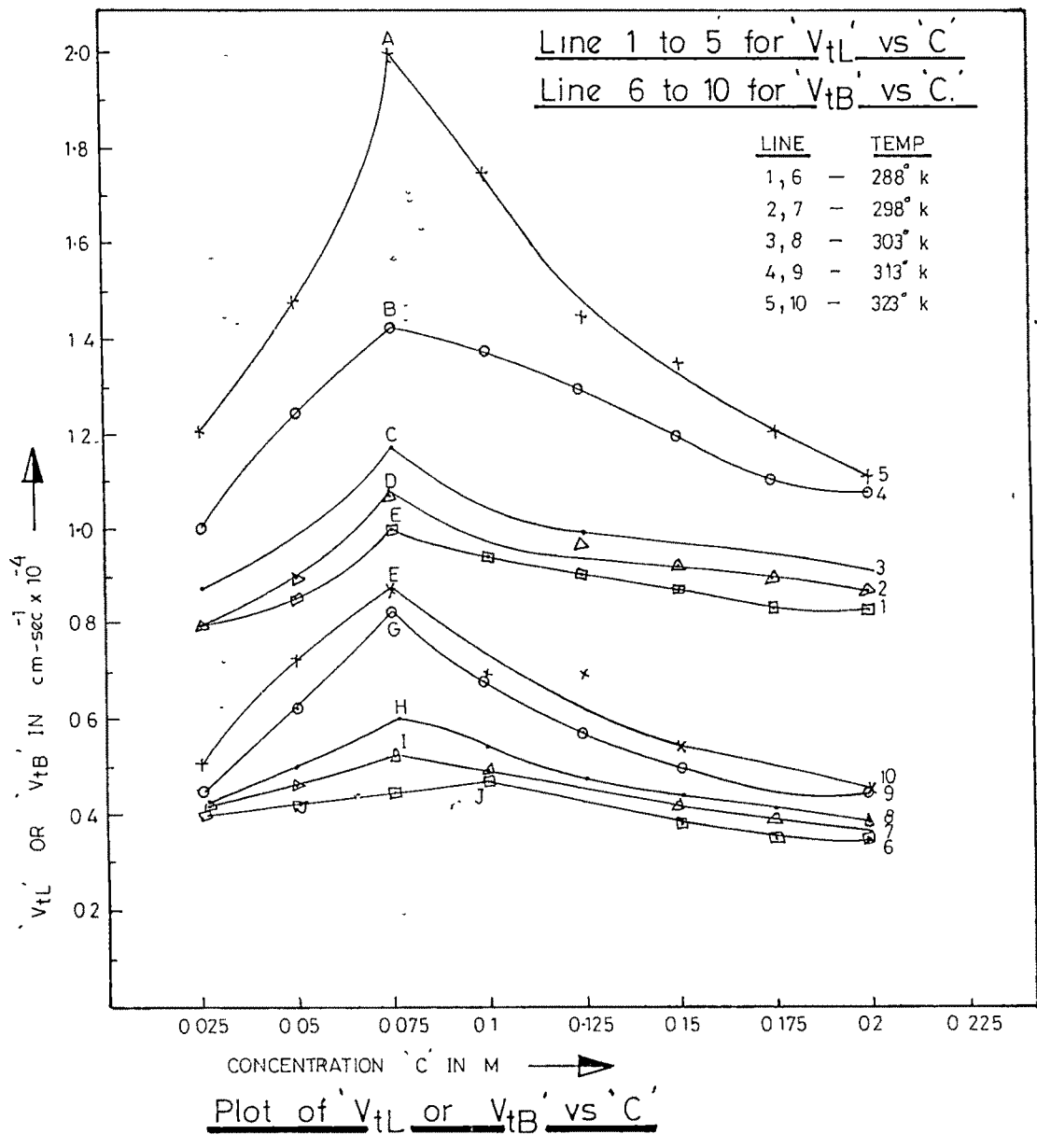
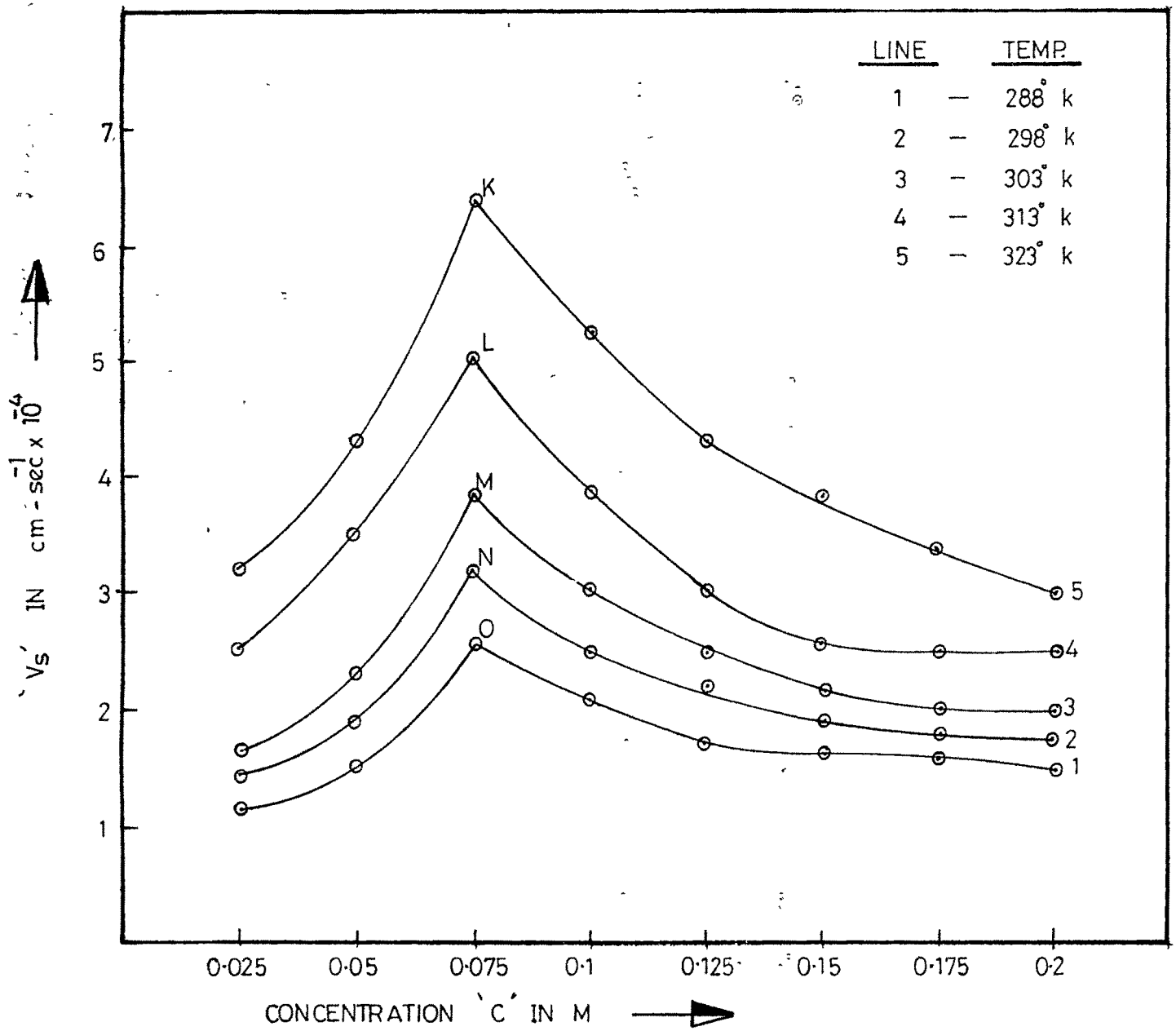
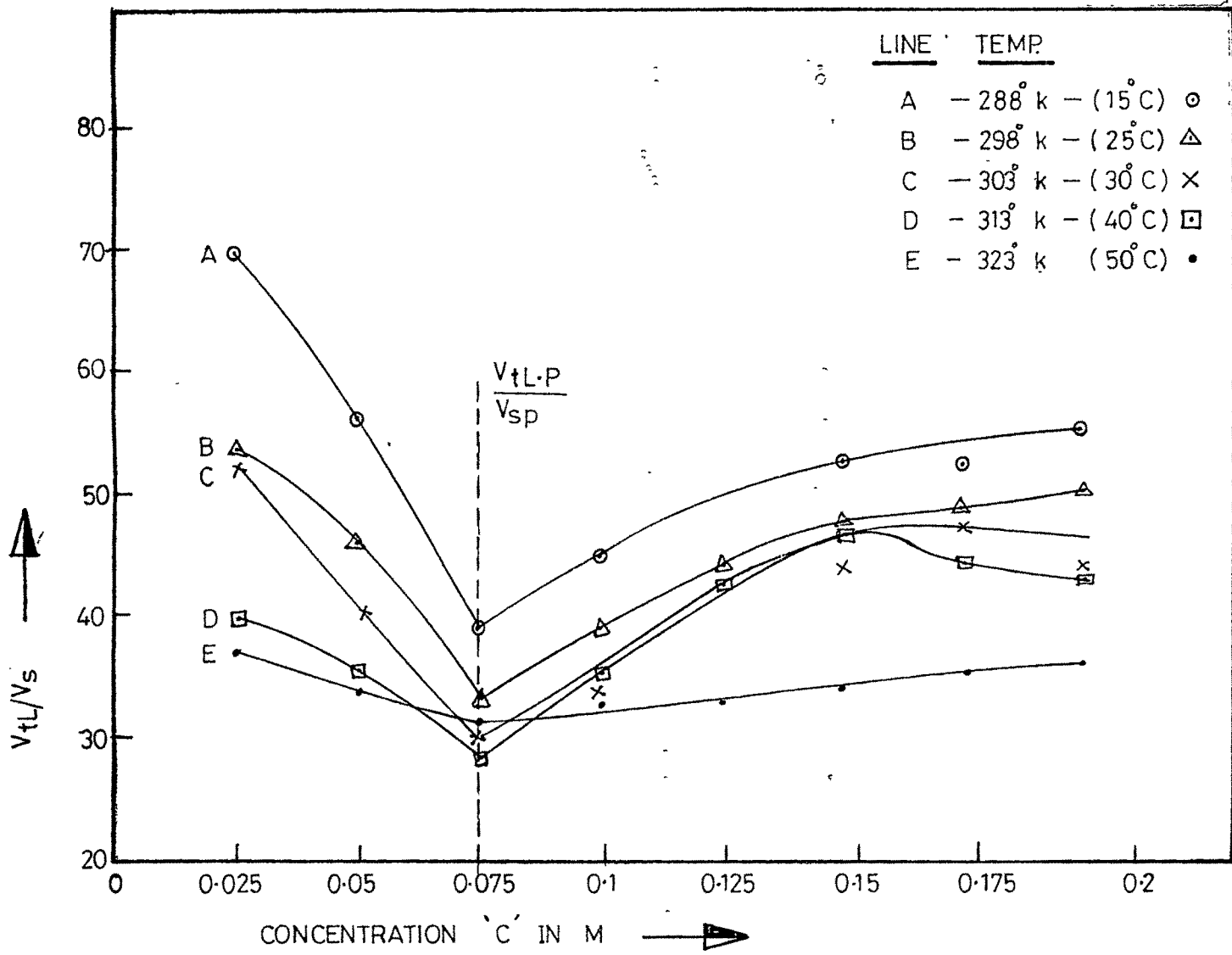


Fig : 9-3



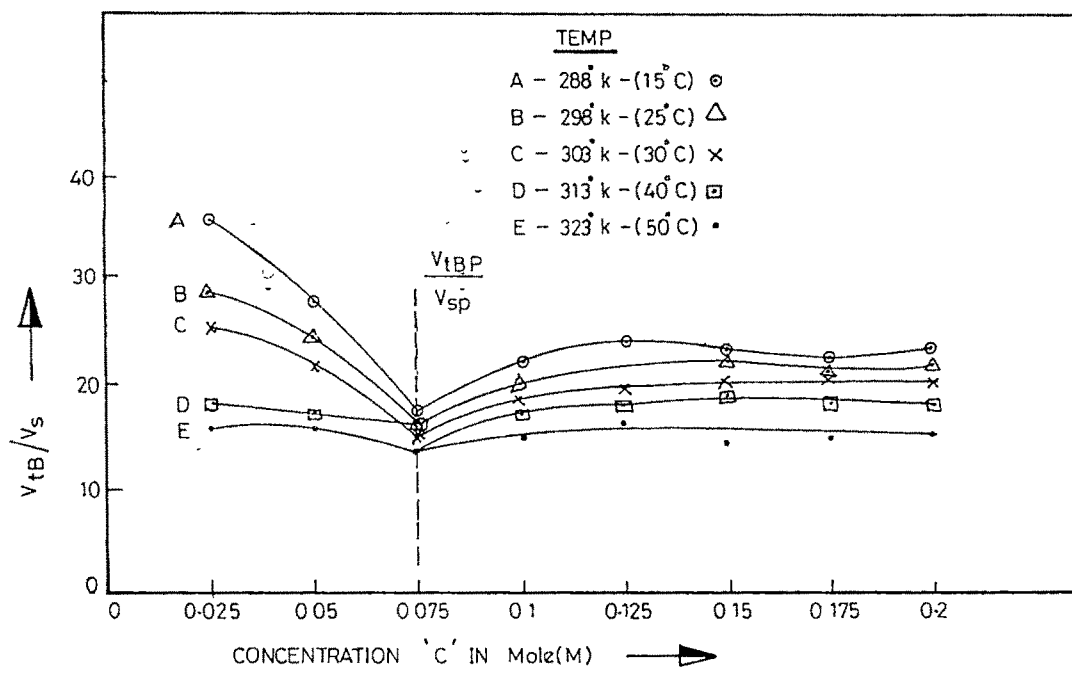
Plot of  $V_s$  vs  $C$ .

Fig. : 9.4



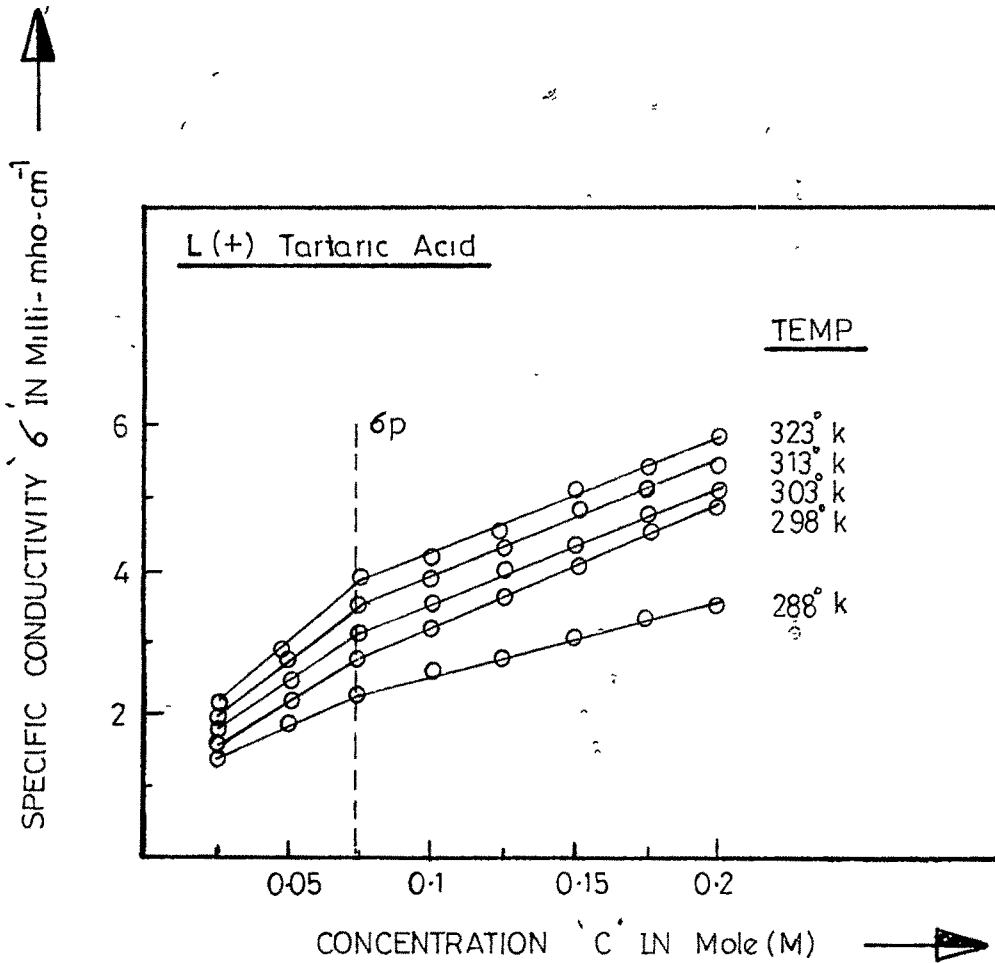
Plot of  $V_{tL}/V_s$  vs  $C$

Fig. : 9.5



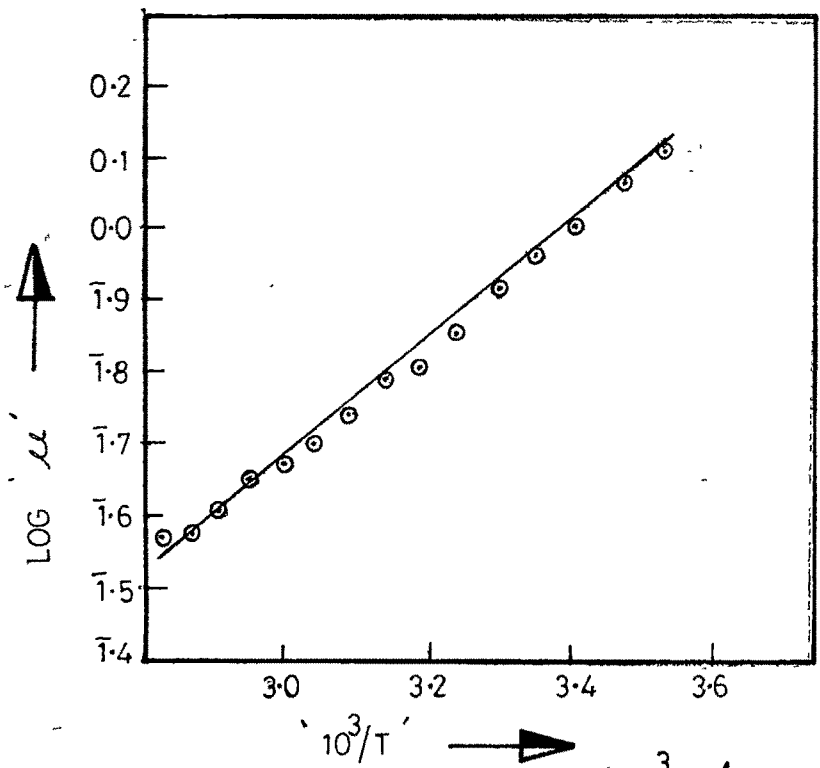
Plot of  $\frac{V_{tB}}{V_s}$  vs 'c'

Fig : 9-6



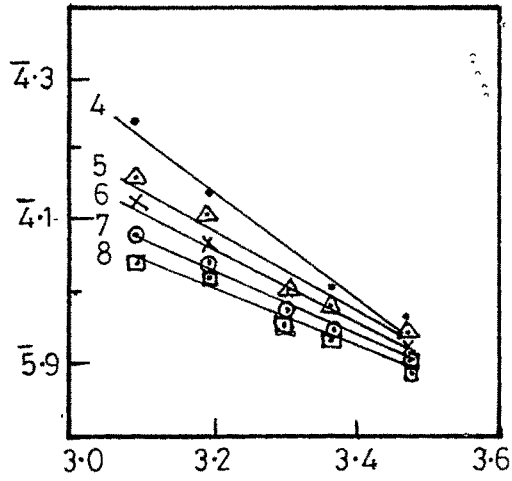
Plot of 'σ' vs 'C'

Fig. : 9.7

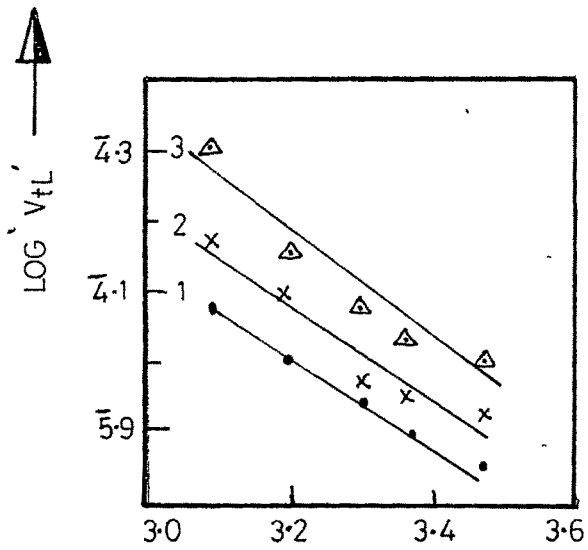


Plot of Log 'μ' vs '10<sup>3</sup>/T' for L(+) Tartaric Acid for 0.025 M, 0.05 M, 0.075M, 0.1 M, 0.125M, 0.15M, 0.175M, 0.2M.

Fig.:9-8

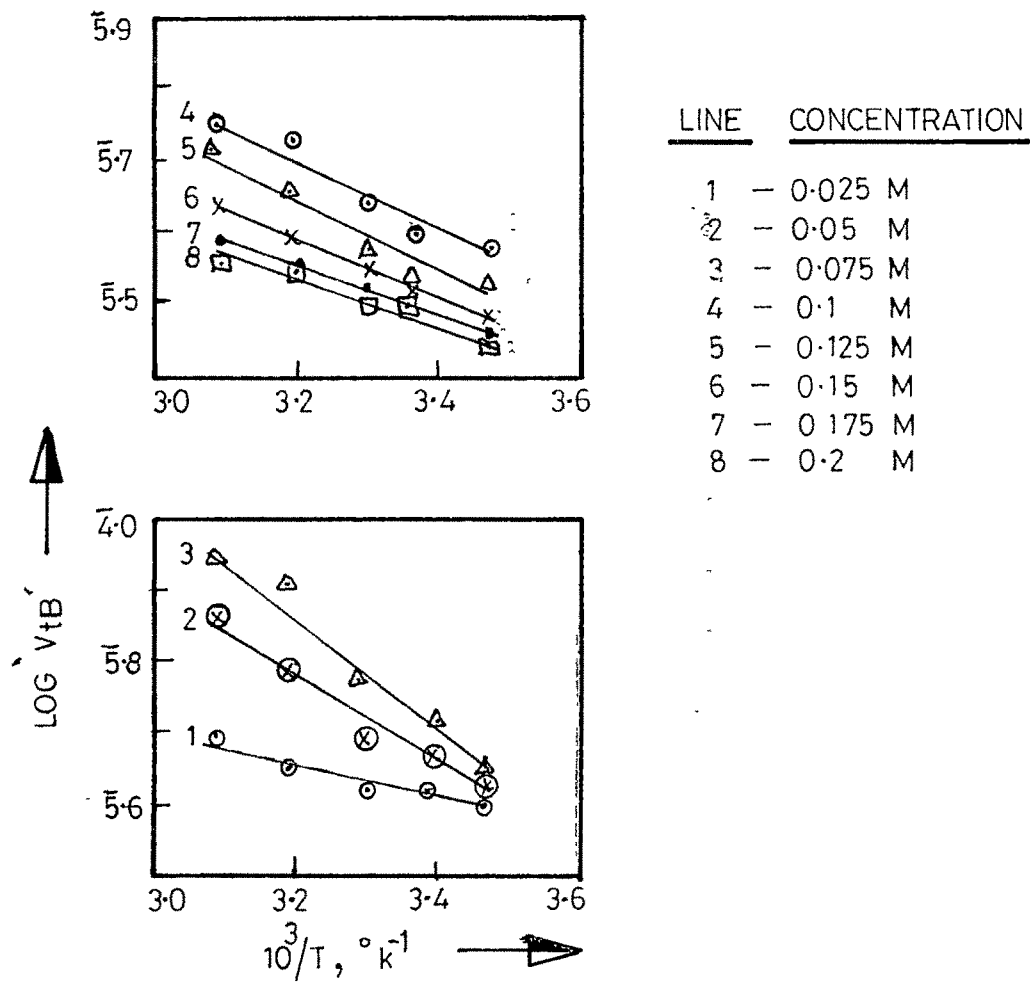


LINE	CONCENTRATION
1	0.025 M
2	0.05 M
3	0.075 M
4	0.1 M
5	0.125 M
6	0.15 M
7	0.175 M
8	0.2 M



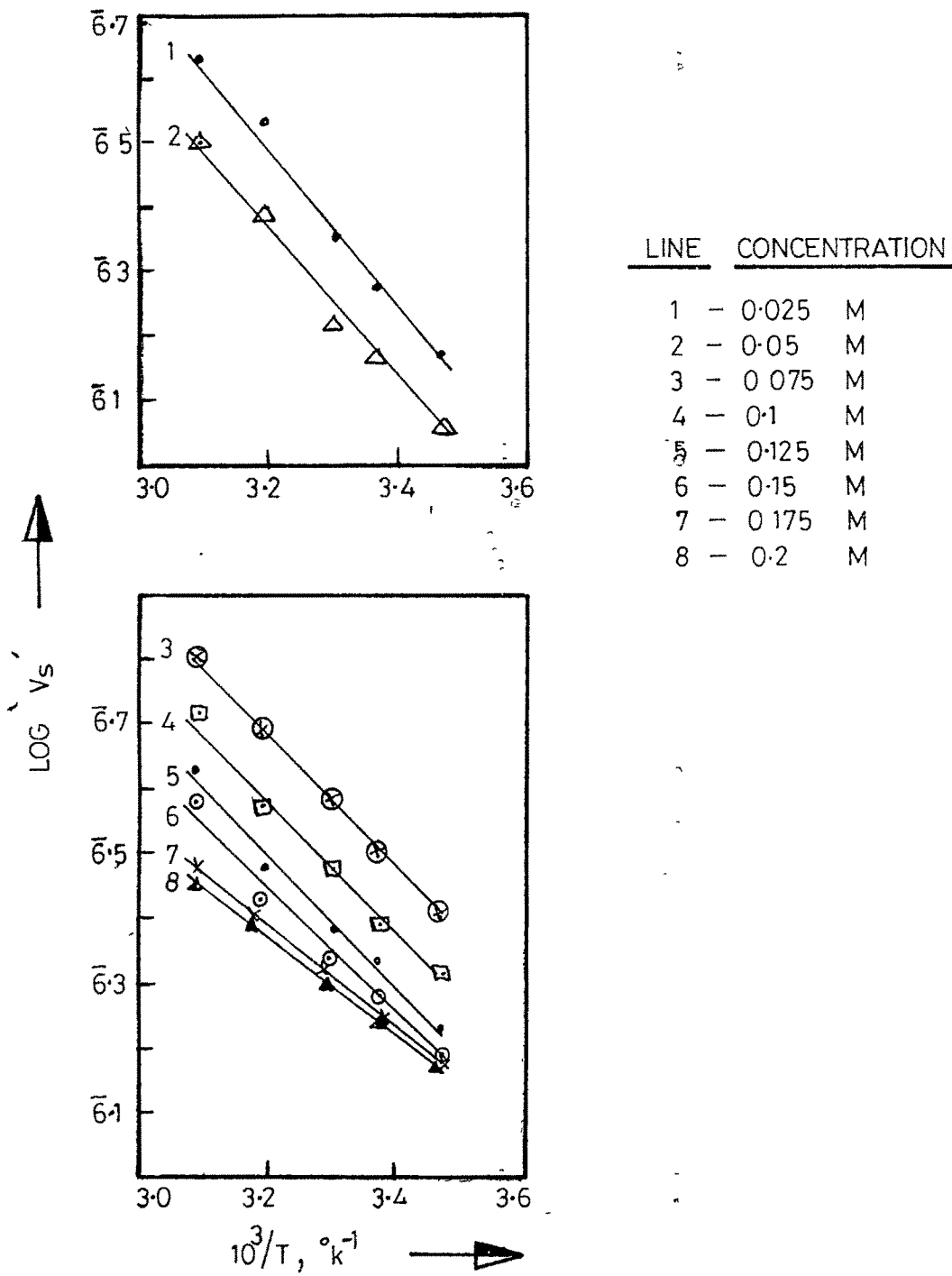
$\text{Plot of } \log V_{tL} \text{ vs } 10^3/T.$

Fig.:9-9



Plot of Log  $V_{tB}$  vs  $10^3/T$ .

Fig. : 9.10



Plot of Log 'Vs' vs '10<sup>3</sup>/T.'

Fig.: 9.11

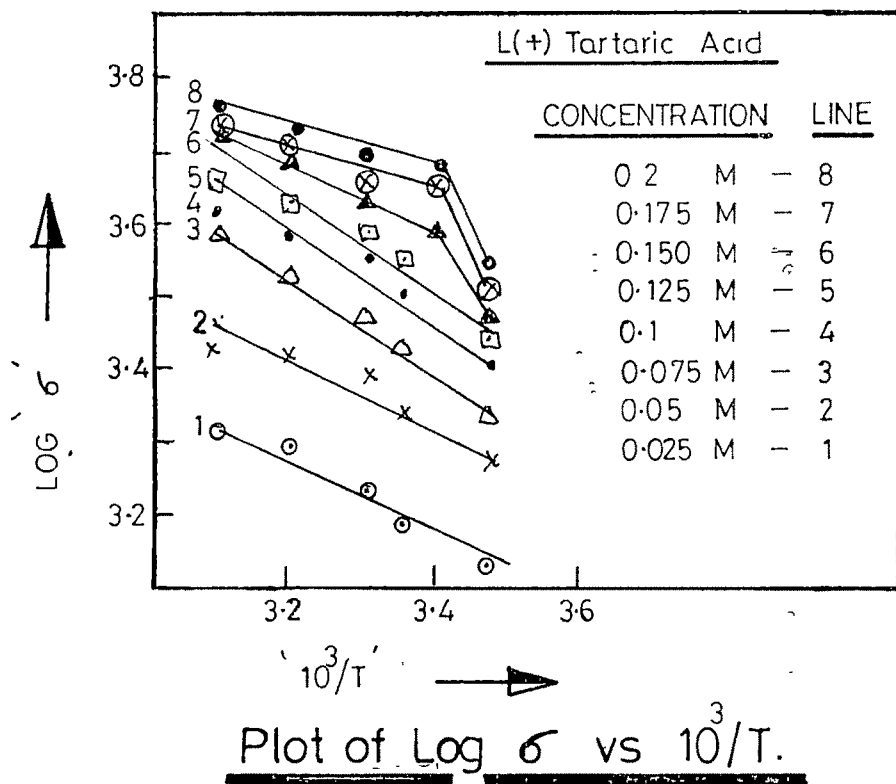


Fig.: 9-12

## REFERENCES

1. Johnston, W.G., J. App. Phys. 27, 1018, (1952)
2. Gilman, J.J., Trans. AIME, 212, 781, (1958)
3. Ives, M.B. and Mcaushand, D.D., Surface Sci., 13, 189, (1963)
4. Ives, M.B. and Hirth, J.P., J. Chem. Phys., 33, 817, (1960)
5. Urusovskaya, A.A., Sov. Phys. Cryst. 10, 437, (1963)
6. Haribabu, V. and Bansigir, K.G., Physica, 30, 2003, (1969)
7. Raju, I.V.K. Bhagvan; Sankaram, T. Bhima, J. Phys. D. 3(12), 1796, (1970)
8. Raju, I.V.K. Bhagvan and Bansigir, K.G., J. Cryst. Growth, 11(2), 171, (1971)
9. Sangwal, K. and Patel, T.C., Kristall and Technik, 13, 281, (1978)
10. Popkova, E.G., Predvoditelev, A.A., Kristallografiya, 15(1), 97, (Russ), (1970)
11. Popkova, E.G., Matveeva, G.S. and Predvoditelev, A.A., 53, (Russ), (1969)
12. Bhatt, V.P., Vyas, A.R. and Pandya, G.R., Ind. J. Pure App. Phys., 12, 807, (1974)
13. Johnston, W.G., Prog. in Ceramic Sci., 33, 21, ed. by J.E. Burke (Pergamon Press) (1962)
14. Robinson, W.H., "Techniques for the Direct Observation of Structure and Imperfections" (John Wiley & Sons, Inc., N.Y.) (1968)
15. Sangwal, K., Etching of Crystals, Theory, Experiment and Application(Defects in Solids, Vol 15)(Elsevier Science Publishers) (1987)
16. Watt, H., Nature (London), 163, 314, (1959)
17. Stanley, R.C., Nature (London), 182, (1958)
18. Pandya, N.S. and Pandya, J.R., Jour. of M.S. University of Baroda, 10, 21, (1961)
19. Mehta, B.J., Ph.D. Thesis, M.S. University of Baroda, Baroda, (1972)

20. Shah, R.T., Ph.D. Thesis, M.S. University of Baroda, Baroda, (1976)
21. Bhagia, L.J., Ph.D. Thesis, M.S. University of Baroda, Baroda, (1983)
22. Shah, A.J., Ph.D. Thesis, M.S. University of Baroda, Baroda, (1984)
23. Hanke, I., Acta. Phys. Austrica, 14, 1, (1961)
24. Patel, A.R. and Tolansky, S., Proc. Roy. Soc. A243, 33, (1957)
25. Pandya, N.S. and Pandya, J.R., Nature, Lond., 184, 894, (1959)
26. Pandya, J.R., Ph.D. Thesis, M.S. University of Baroda, Baroda, (1961)
27. Sangwal, K. and Arrora, S.K., J. Mat. Sci., 13, 1977, (1978)
28. Sangwal, K.; Patel, T.C. and Kotak, M.D., Kristall and Technik, 14, 8, 949, (1979)
29. Gerasimov, Ya; Dreving, V.; Kiselev, A.; Eremin, E.; Shlygin, A. and Panchenkov, G., Physical Chemistry Vol.2, Mir Publishers, Moscow, (1974)
30. Gilman, J.J., Surface Chemi. Metals and Semi-conductor Symp., John Wiley & Sons, N.Y. (1960)
31. Ives, M.B. and Plew, J.T., J. Chem. Phys. 42, 293, (1965)
32. Laidler, K.J., Chemical Kinetics, McGraw Hill Book Co., (1950)
33. Bogenschultz, A.F.; Locherer, K. and Mussinger, W., J. Electrochem. Soc., 114, 970, 1967.
34. Abramson, M.S. and King, C.V., J. Amer. Chem. Soc., 61, 2290, (1939)